Structural Analysis of the Controlled Impact Demonstration of a Jet Transport Airplane

Edwin L. Fasanella*
PRC Kentron, Hampton, Virginia
E. Widmayer†
Boeing Commercial Airplane Company, Seattle, Washington
and
Martha P. Robinson‡
NASA Langley Research Center, Hampton, Virginia

In 1980 NASA Langley Research Center and the Federal Aviation Administration began an extensive research and development program to quantitatively assess transport airplane crashes. As part of this program, a survivable, full-scale crash test of a transport airplane was planned. On December 1, 1984, the FAA, NASA and industry contractors conducted a remotely piloted crash test using an out-of-service Boeing 720 jet transport airplane. A major purpose of the test, designated the Controlled Impact Demonstration is to advance analytical modeling techniques for simulating transport crash dynamics. This paper describes NASA analyses using the nonlinear finite-element computer code Dynamic Crash Analysis of Structures. The research is described beginning with transport fuselage section drop tests and single frame models, culminating with finite-element models of the Boeing 720 airplane. The final model based on test and analysis, simulates the Controlled Impact Demonstration impact with excellent correlation.

Introduction

As part of an effort to study transport crash safety, a series of three transport fuselage section drop tests at impact velocity 20 ft/s were conducted[1,2] at NASA Langley Research Center's Impact Dynamics Facility. These tests provided data to qualify instrumentation and to test impact tolerance of data acquisition hardware in preparation for the Controlled Impact Demonstration (CID). In addition, the data from the section drop tests[3] were compared with the DYCAST[4] computer model predictions, and used to develop nonlinear subfloor crush springs for a hybrid finite-element airplane model used to evaluate pre-CID impact scenarios and to simulate the actual CID test. The Federal Aviation Administration (FAA) conducted an additional drop test at 17 ft/s of a complete Boeing 707 airplane providing valuable crush and damage information which was useful in the modeling effort.

The FAA initiated the CID program for two reasons: 1) to test an antimisting kerosene fuel, and 2) to study structural crashworthiness. NASA Langley Research Center's responsibilities were to build the data acquisition system, collect and analyze the data from the 350 transducers on board,[5-7] conduct crashworthiness experiments, provide onboard film coverage, and perform finite-element modeling. Boeing Commercial Airplane Company provided assistance for the finite-element modeling of the Boeing 720 airplane. NASA Ames Dryden Flight Research Facility developed the flight program and remotely piloted the airplane to the impact site.

This paper describes NASA research in modeling transport airplane structure using DYCAST. The analysis starts with simple frame and fuselage section models, and progresses to a full Boeing 720 hybrid model used to simulate the CID. Comparisons of experimental and analytical results from this research are presented. Other modeling using the program KRASH is presented in Ref. 8.

DYCAST Analytical Program

DYCAST is a nonlinear structural dynamic finite-element computer code developed by Grumman Aerospace Corporation with principal support from NASA and the FAA. The element library consists of the following: 1) stringers, 2) beams, 3) membrane skin triangles, 4) plate bending triangles, and 5) spring elements. The spring element can be either elastic or dissipative and is useful to model the crush behavior of components for which data are available and whose behavior may be too complex to model otherwise.

Changing stiffnesses in the structure are accounted for by plasticity and very large deflections. Material nonlinearities are accommodated by one of three options: 1) elastic-perfectly plastic, 2) elastic-linear hardening plastic, or 3) elastic-nonlinear hardening plastic of the Ramberg-Osgood type. The second option has been used exclusively for this modeling effort. Geometric nonlinearities are handled in an updated Lagrangian formulation by reforming the structure into its deformed shape after small time increments while accumulating deformations, strains, and forces. The nonlinearities due to combined loadings are maintained, and stiffness variations due to structural failures are computed. The failure option is imposed automatically whenever a material failure strain criterion is met, or manually by the user at a restart.

Other features include multiple time-load history tables to subject the structure to time dependent loading; gravity loading; initial pitch, roll, yaw, and translation of the structural model with respect to the global system; a bandwidth op-

Received April 30, 1986; presented as Paper 86-0939 at the AIAA/ASME/ASCE/AHS 27th Structures, Structural Dynamics and Materials Conference, San Antonio, TX, May 19-21, 1986; revision received Oct. 27, 1986.

*Supervisor, Structures Support Unit.
†Principal Engineer.
‡Aerospace Technologist.

timizer as a preprocessor; and deformed plots and graphics as postprocessors.

Numerical time integrators available are central difference, modified Adams, Newark-beta, and Wilson-theta. The Newark-beta integrator was used exclusively for the models presented in this paper.

Controlled Impact Demonstration Airplane

The aircraft used in the CID was a mid-1960 Boeing 720, four-engine, intermediate range, jet transport (see Fig. 1). Although the Boeing 720 is now considered obsolete, its structural design and construction are still representative of narrow-body transport aircraft currently in use. In preparation for the CID test, several fuselage sections were drop tested. Because of the difficulty in locating a Boeing 720, nearly identical 707 fuselage sections were used for test specimens.

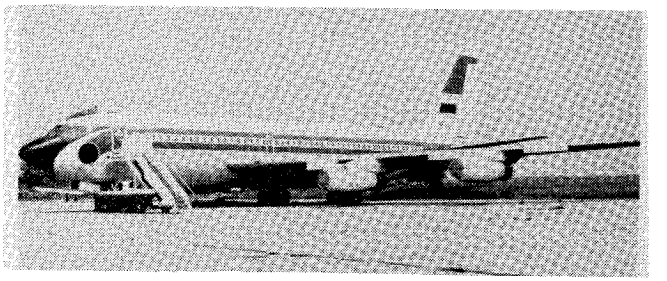

Fig. 1 Boeing 720 transport used in CID.

Forward Fuselage Section

Figure 2 shows a forward fuselage section suspended in a drop tower at the NASA Langley Research Center. The 12-ft long fuselage section weighed 5051 lb including the seats, anthropomorphic dummies, and instrumentation.[9] The structural beams and paneling of the lower bulkhead, closing off the cargo bay, were removed to make the subfloor structural strength more uniform lengthwise.

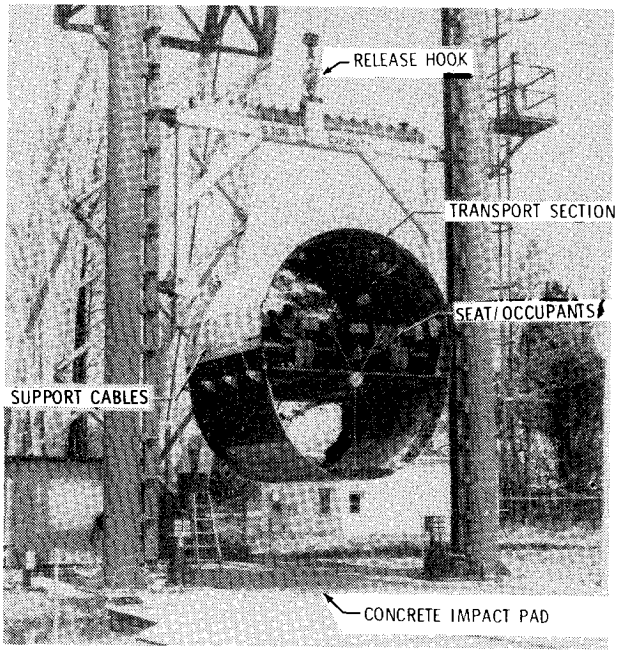

Fig. 2 Forward transport section in drop tower.

Modeling Considerations

Various structural failure mechanisms must be accommodated analytically to accurately model structural behavior. For example, the lower lobe of the fuselage section resists vertical loading through deformation of the frames, whereas the longitudinal stringers and skin offer little resistance to crush. The lower frames could be expected to fail in bending and/or in shear and potentially to develop points of inflection and "snap through" due to ground reaction forces. The ground reaction might also impose high transverse shear loads on the frame cross sections. In addition, plastic hinges might develop in the frames between the floor level and the fuselage bottom. If the frames do not rupture while undergoing these types of deformations, large impulsive moments will be applied to the floor and the upper frame. Thus, the analytical formulation needs to provide for many basic failure mechanisms.

At the current level of crash analysis and computer resources, it is necessary to judiciously limit the number of degrees of freedom (nodes) and the number of structural elements in the model. As the degrees of freedom increase, model debugging, verification of the dynamic behavior, and interpretation of the results become increasingly difficult. Consequently, it is desirable to understand the behavior of less complicated components prior to formulation of the complete structural model.

Single Frame Model

The single frame half-model took advantage of symmetry about the fuselage center line. The frame was constrained to in-plane deflections with boundary conditions applied at crown, floor, and keel. The half-frame model had 62 nodes, 102 elements, and 103 degrees of freedom. Variations of the frame cross sections from crown to keel were modeled. The DYCAST offset beam capability allowed proper behavior of multiple beams connecting two nodes. Individual elements could be monitored during plastic deformation and rupture. The frame model results provided significant insight into dynamic responses of the floor and upper lobe, and identified problems and solutions with snap-through of the lower frame and shear failure of the frame web near the fuselage bottom.

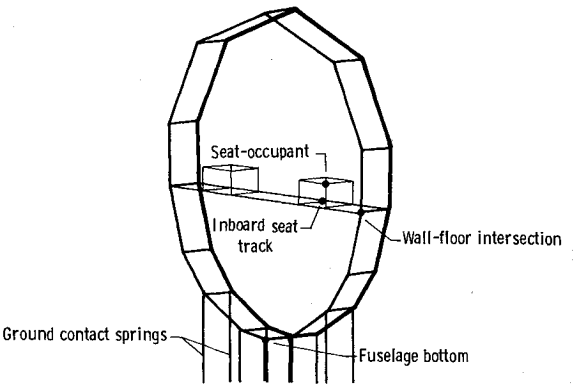

Fig. 3 Two-frame model showing nodes where responses are compared.

On the basis of frame predictions, approximations of the lower fuselage crushing characteristics were obtained which permitted simplifications of the fuselage structure that was particularly useful in the CID airplane model. Frames below the floor level could be represented as a single vertical spring having known force-deflection characteristics; thus, many finite elements could be replaced with a single hybrid spring element to reduce the problem to manageable size.

Two-Frame DYCAST Model

A two-frame model with sufficient detail to model the floor, two seats with lumped mass occupants, and the fuse-

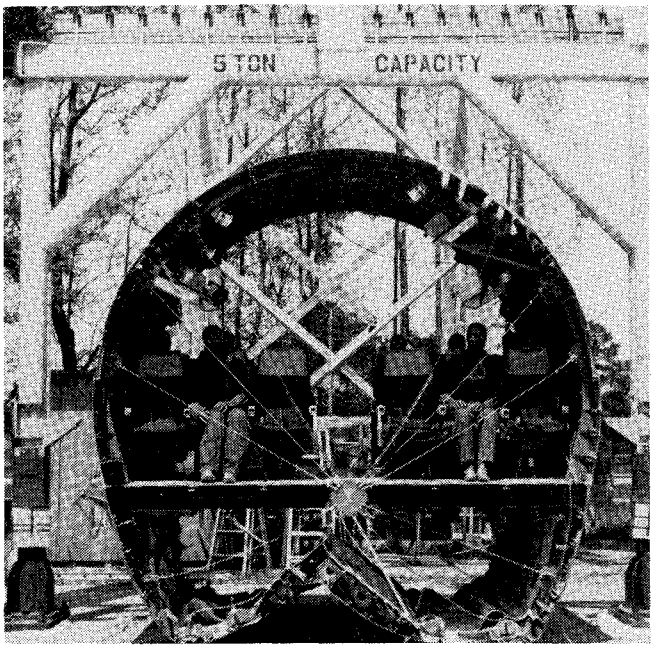

Fig. 4 Forward transport section showing post-test damage.

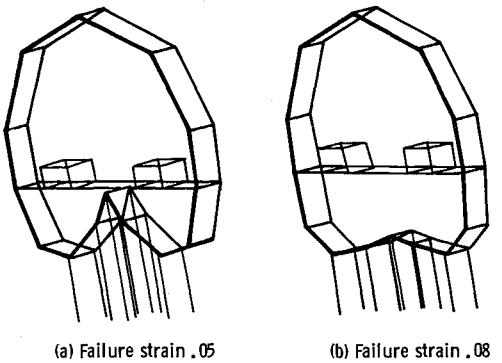

Fig. 5 Effects of beam failure strain at time 0.23 s after impact.

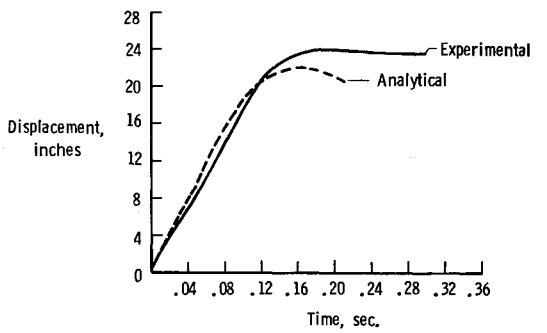

Fig. 6 Comparison of vertical floor displacements.

lage structure without using nonlinear springs (except for the seat and ground properties) was formulated. Although symmetry was lacking for the full section, the two forward frames and seats did exhibit a vertical plane of symmetry. Thus a symmetric, two-frame, half-model was used for computations on the section.

The two-frame model is shown schematically in Fig. 3. Stiff ground springs simulated the concrete pad impact surface. Each frame of the lower fuselage below the floor was modeled using eight beam elements. Floor and seat rails were modeled using appropriate beam elements. The fuselage structure above the floor (not expected to deform plastically) was modeled in less detail to keep the model as small as possible. The triple seat/occupant model consisted of four lumped masses connected by horizontal stringer elements supported by four nonlinear springs representing the vertical legs. The mass of the three occupants was distributed using a 2 to 1 ratio with inboard seat legs supporting two occupants and outboard legs supporting only one occupant due to asymmetry of the seat pan with respect to the legs.

To simulate end constraints and strengthen the section, motion was not allowed in the fore-and-aft (x-axis) direction. Initially, the time step was allowed to vary, but was later held constant to 250 μs to correspond to the sample rate (4000/s) used to digitize the experimental accelerations. Consequently, the same digital low pass filter used to filter the experimental data could be used to filter the DYCAST calculated accelerations without requiring an interpolation algorithm before filtering. The 250-μs time step was conservative for this problem compared to a minimum time step of 500 μs when a variable time step was allowed in an earlier run. To run 901 constant time increments (0.225 s total) required 1620 CPU s on a CDC Cyber 175.

Figure 4 illustrates the structural behavior/damage experienced by the fuselage section during the vertical impact test at 20 ft/s. The gross structural damage was primarily confined to below the floor level. All seven frames ruptured near the bottom contact point. Plastic hinges formed in each frame along both sides of the fuselage. Static crush measured from floor level varied from 22–23 in. for the forward end to 18–19 in. for the rear.

Nonlinear material properties used for the critical subfloor aluminum frame beam elements were elastic-plastic with a small amount of linear strain hardening. The yield stress initially chosen was 83,000 psi with a failure strain of 11%. However, the DYCAST model was too strong using this yield stress and failure stain and did not predict sufficient crush. When using elements to represent macrosections of structure, the elongation to failure is difficult to determine due to stress risers, section changes, etc. Although material coupon tests may show 11–13% elongation, failure generally occurs much earlier when material is fabricated into large structure. In addition, data from tests of large panels of aircraft structure indicate that yield is typically in the 40–50,000 psi range.

As a consequence, the aluminum beam yield stress in the model was reduced to 50,000 psi and failure strain was set to 5%. Effects of the beam failure strain criteria in DYCAST on the two-frame model are shown in Fig. 5 for 0.23 s after impact. The beam failure criteria for the two-frame model were conservative since the entire beam failed when one Gaussian integration point reached the specified maximum normal strain. With a failure strain of 5%, beams at the bottom of the fuselage failed too soon and excessive deformation of the structure was predicted. To overcome the early failure, the maximum strain was increased to 8% for better simulation. As a result of this problem, DYCAST was later modified to include a partial beam failure criteria. Partial element failure is obtained when the specified failure strain is reached locally. The material stiffness corresponding to that integration point is set to zero. An element is deleted only when all integration points reach the specified failure strain.

For a yield stress of 50,000 psi and failure strain of 8%, good correlation with the experiment was achieved; thus these values were used in the two-frame model for all comparisons with experimental data. Figures 6–10 present a comparison of vertical experimental and analytical floor displacements, dummy pelvis accelerations, and accelerations of the fuselage section at the ground contact point, wall-floor intersection, and inboard seat track. Comparisons are good for the fuselage crushing and the accelerations of the floor fuselage. The seat and occupant model was adequate to approximate dynamic loading to the floor, but a more

sophisticated model would be required for good correlations with dummy accelerations.

Although a full section model using only finite elements for subfloor was desirable, constraints of time and computer resources limited the finite-element subfloor model of the forward section to a two-frame model. Comparisons of experimental data with results from the two-frame model indicate that DYCAST can provide excellent correlation with the impact behavior of the fuselage structure with a minimum of empirical force-deflection data representing the structure in the analytical model.

Aft Section DYCAST Model

A Boeing 707 aft fuselage section weighing 6395 lb was also drop tested at 20 ft/s.[10] The aft section lower lobe is not a constant cross section like the forward section but tapers upward toward the rear. A cargo door further disrupts lower body symmetry. Because of asymmetry, a full fuselage section model was necessary. Several design iterations reduced the model to 650 degrees of freedom and 241 elements (Fig. 11). To further reduce the model size the crown was modeled with a limited number of elements. Vertical ground reactions were provided using seven springs at each frame. For simplicity each stringer-skin combination was lumped into a beam element. A seat with three occupants and an instrumentation data acquisition pallet were modeled using springs and lumped mass. Displacements predicted by the model were approximately 23 and 27 in., respectively, for the front corners and for the rear floor. Measured displacements were approximately 18 in. for the front and 26 in. for the rear. Typical predicted peak floor accelerations indicated an initial peak of 8–10 *g* corresponding to the loading and failure of the lower lobe and a second peak of approximately 20 *g* representing reloading of the structures. Measured values were 8–10 for the first peak, and somewhat less than 20 *g* for the second. A computer plot of the deformed aft section for time 0.1649 s is shown in Fig. 12.

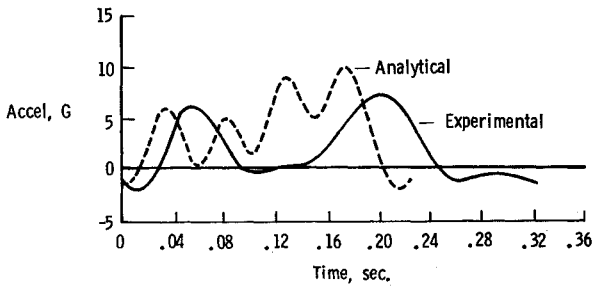

Fig. 7 Comparison of vertical pelvis accelerations.

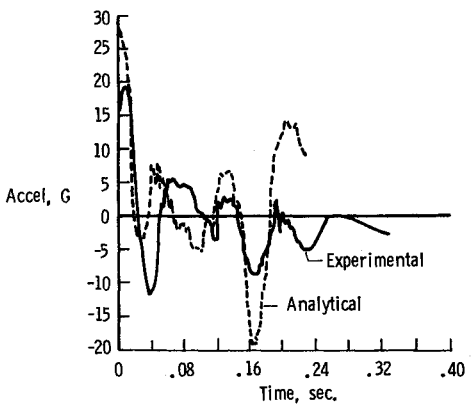

Fig. 8 Comparison of vertical accelerations at ground contact point.

Controlled Impact Demonstration

A plan view of the CID is shown in Fig. 13 with longitudinal body station (BS) locations labeled and compared to the distance (in in.) from the nose of the aircraft (*x*-coordinate). A study[11] by NASA, FAA and three major U.S. airframe manufacturers was conducted to determine a typical "impact survivable" accident. In addition, the FAA required fuel spillage and ignition sources to test the antimisting kerosene fuel.

The planned CID scenario resulting from these studies is illustrated in Fig. 14. The Boeing 720 was to follow a 3.3–4.0-deg glide slope in a 1-deg nose-up attitude. The aircraft was to have a 17 ft/s sink rate and a longitudinal velocity of approximately 150 knots. After the primary impact, the airplane fuselage was to slide between a corridor of wing openers to cut the wing tanks and insure spillage of 20–100 gal of fuel/s. The structural crashworthy experiment would be completed before the airplane contacted the wing openers.

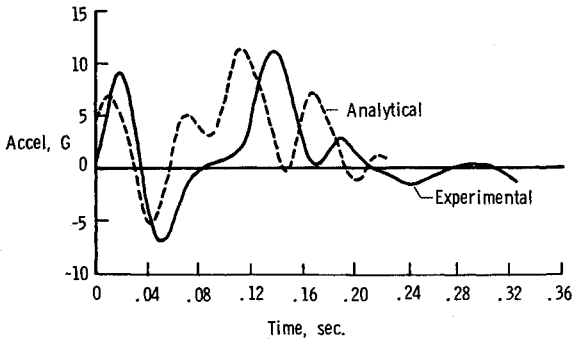

Fig. 9 Comparison of vertical accelerations at wall/floor interface.

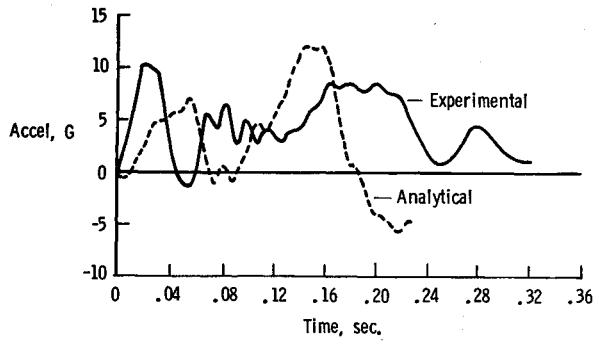

Fig. 10 Comparison of vertical accelerations of inboard seat track.

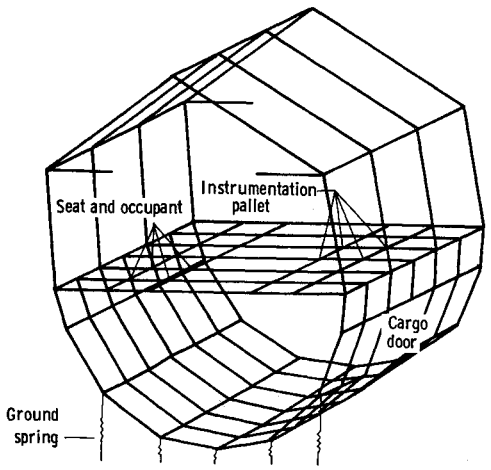

Fig. 11 Aft transport section model.

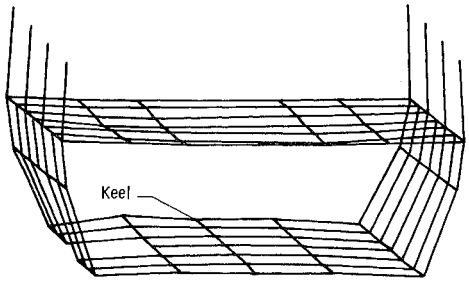

Fig. 12 Aft transport section model at time 0.1649 s after impact.

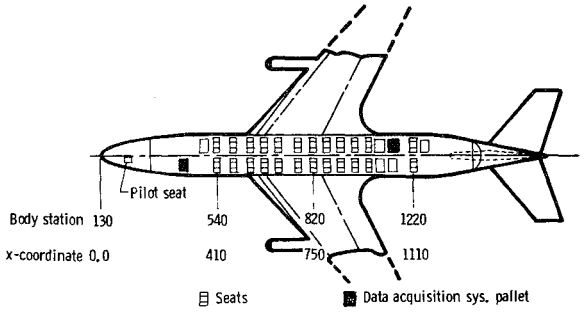

Fig. 13 CID floor layout.

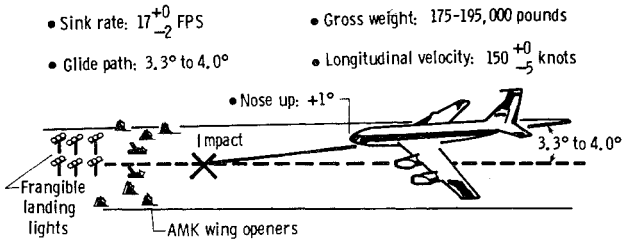

Fig. 14 CID planned impact scenario.

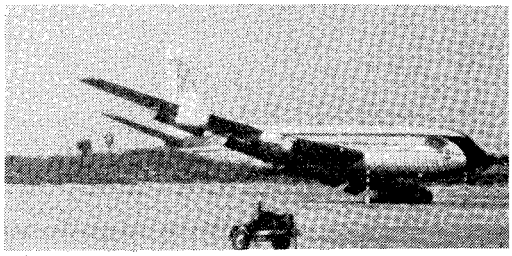

Left wing impact

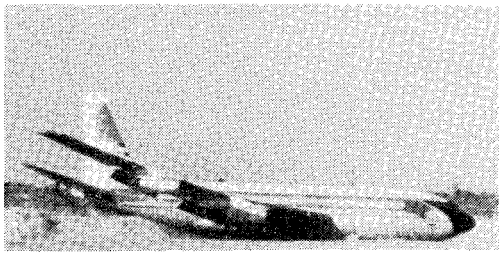

Fuselage impact

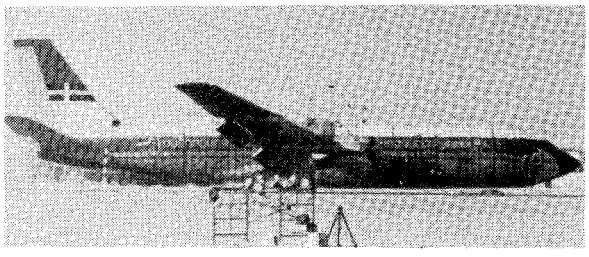

Impact with wing openers

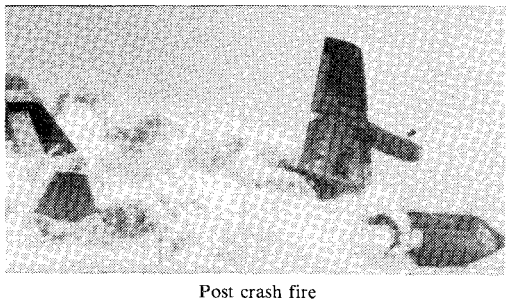

Post crash fire

Fig. 15 CID impact sequence.

In the actual impact the outboard number 1 engine on the left wing contacted the ground first as a result of a 13-deg roll and yaw, and zero-deg pitch (see Fig. 15). The gross weight of the airplane at impact was estimated to be 192,000 lb. At the time of wing contact, the airplane c.g. sink rate was approximately 17 ft/s and the horizontal velocity was 248 ft/s. The impact and drag force on the wing caused the airplane to develop an angular velocity about the pitch axis. Approximately 0.5 s after the left wing impacted the ground, the forward fuselage impacted the ground behind the nose gear wheel well. The pitch attitude of the airplane at nose impact was about −2.5 deg. Figure 16 shows the pitch history measured from film analysis beginning with wing contact.

The left wing impact and wing crush significantly influenced the crash dynamics of CID and the subsequent fire damage obliterated the crush at the rear of the airplane. From an analysis of integrated vertical acceleration traces, it is estimated that the c.g. velocity was reduced from 17 ft/s at left wing contact to about 12 ft/s at nose impact. The angular pitch rate at nose impact measured about the c.g. was about −0.1 rad/s. Highest vertical velocities were forward of the c.g.

DYCAST Modeling of the CID

Since the CID impact was planned to be as nearly symmetric as possible, the DYCAST Boeing 720 model developed was a symmetric half-model. In addition, the wing model and the forward cabin were not as well defined as the rear of the fuselage where initial impact was expected. After the CID test, the model was modified and additional crush springs were added in the forward cabin.

Fuselage contact occurred 0.46 s after left wing (engine number 1) contact. Model predictions begin at fuselage contact with ground and continue for 0.15 s. Initial conditions used in the DYCAST analysis were 12 ft/s vertical velocity at the c.g., −0.1 rad/s pitch rate, and an initial pitch of −2.5 deg at the time of fuselage impact. Yaw and roll conditions were ignored for this analysis. To introduce the pitch rate into DYCAST, the initial velocity of each node was computed using

$$v = v_{c.g.} + (\omega \times R) \tag{1}$$

where ω is the pitch rate in rad/s; $v_{c.g.}$ is the velocity vector of the center of gravity; and R the vector from the c.g. to the node.

The CID model at time zero (initial fuselage contact) is shown in Fig. 17. The fuselage bottom initial ground contact point at BS 488, behind the rear nose gear bulkhead, was positioned just above the ground. The model consists of 126 beams, 73 structural crush springs, 15 ground springs, 113 concentrated masses, 196 independent degrees of freedom, and 68 dependent degrees of freedom (see Fig. 18). External

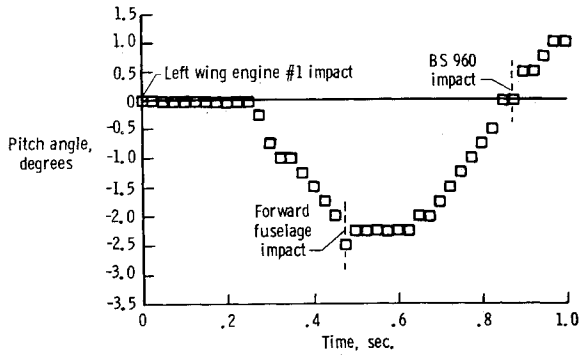

Fig. 16 CID pitch history for first second after left wing contact.

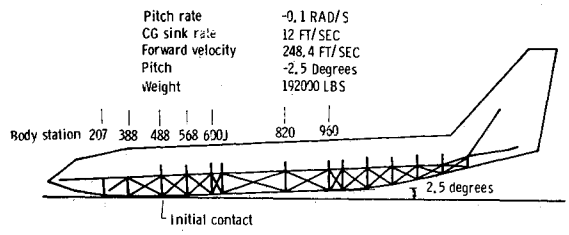

Fig. 17 CID model attitude and conditions at initial fuselage ground impact.

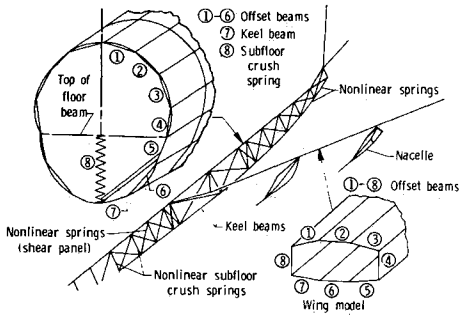

Fig. 18 CID airplane model.

forces acting on the model are gravity, friction, and time dependent lift and wing crush forces. A vertical wing crush force was needed because of the inadequacy of the simple wing model to predict progressive rupture of the wing structure. The wing was modeled using eight tapered offset beams as shown in Fig. 18. A typical fuselage cross section is also shown in Fig. 18. Six offset beam elements constrained to the motion of a reference element on the plane of symmetry at floor level represent the fuselage bending properties. The keel is represented by a beam in the center section and as springs in the remainder of the aircraft. The diagonal springs represent the shear resistance of the fuselage skin. Vertical springs were used to model the lower fuselage crush properties developed from analysis of single frames and section tests.[2]

The model required 1641 s on a CYBER 175 to run 0.15 s in real time. With the airplane pitched as shown, BS 960 at the rear main landing gear bulkhead is about 27 in. off the ground. The time sequence of ground contact was BS 488 at time zero; BS 388 at 0.01 s; BS 302 and BS 568 at 0.035 s; BS 600J at 0.075 s; and BS 620 at 0.100 s. By 0.15 s, most of the aircraft vertical energy was absorbed. In the experimental data, BS 960 makes ground contact about 0.4 s after the initial ground contact. However, the vertical acceleration at the floor level was only 2 or 3 g.

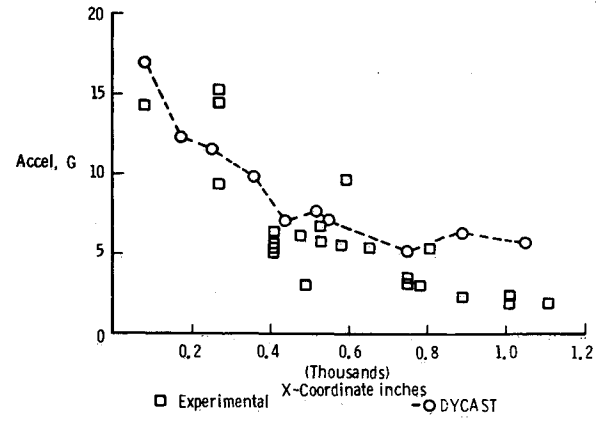

Fig. 19 Comparison of peak vertical floor accelerations.

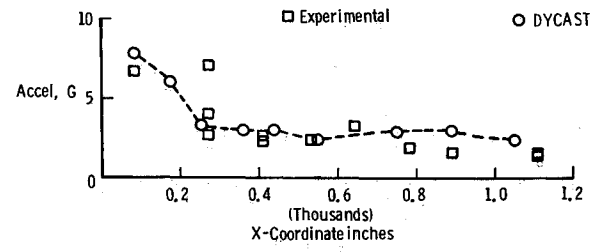

Fig. 20 Comparison of peak longitudinal floor accelerations.

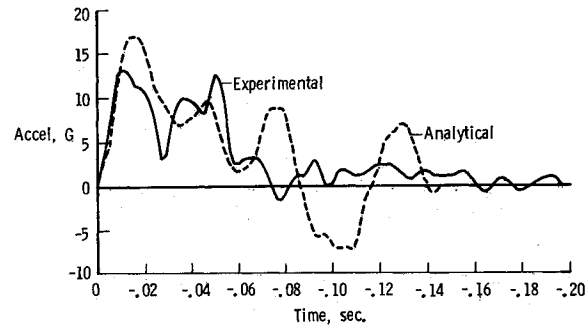

Fig. 21 Comparison of vertical floor accelerations at BS 207.

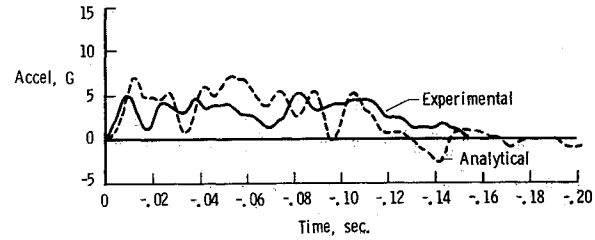

Fig. 22 Comparison of vertical floor accelerations at BS 540.

Figures 19–20 show analytical DYCAST and experimental CID vertical and longitudinal floor peak accelerations as a function of the fuselage x coordinates. The x-axis origin was located at the aircraft nose. Both experimental accelerations and DYCAST predictions have been filtered with a 100-Hz digital filter. The comparisons are considered good although a symmetric model was used with roll and yaw neglected. Figures 21–24 compare CID experimental and DYCAST acceleration time histories for floor locations near the pilot, BS 540, BS 600J, and BS 820. DYCAST slightly overpredicts the

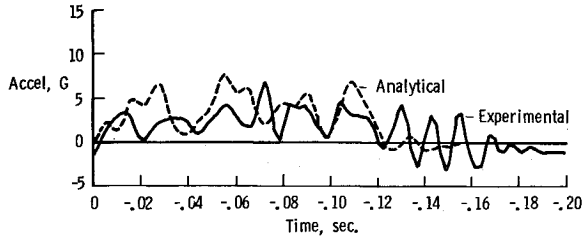

Fig. 23 Comparison of vertical floor accelerations at BS 600J.

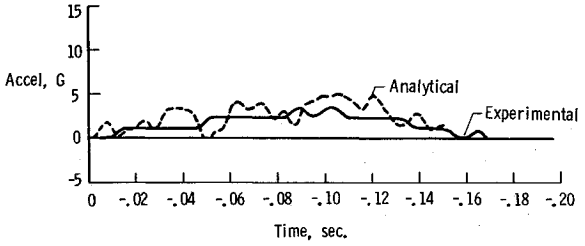

Fig. 24 Comparison of vertical floor accelerations at BS 820.

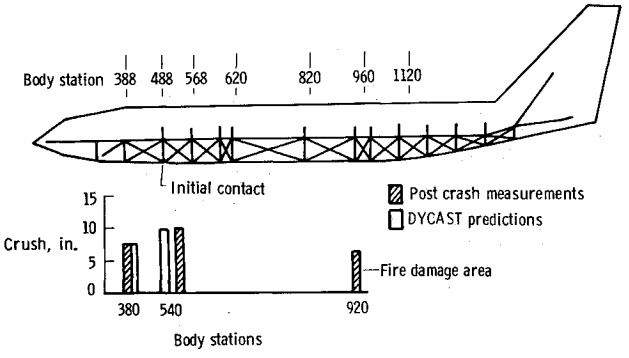

Fig. 25 Comparison of post-crush measurements with DYCAST predictions.

peak accelerations, but the basic waveform of the acceleration matches the experimental acceleration pattern well.

Figure 25 shows a comparison of measured fuselage crush versus DYCAST predicted crush for forward fuselage locations. The wing cutters ripped out the center section keel beam and post crash fire destroyed the aft end of the aircraft; thus measurements past the center of the aircraft cannot be assessed for initial impact. Correlation of the DYCAST model predictions with the experimental structural accelerations and crush data was good for the forward fuselage.

Subsequent analyses will include a full, asymmetric airplane simulation which will allow parametric studies of pertinent impact parameters to be conducted. Although the validation of the DYCAST model using CID experimental results does not include major fuselage structural breakup, crash scenarios will be used which could cause major structural breakup.

Concluding Remarks

DYCAST has been used in a series of progressively more difficult modeling tasks with the goal of accurately modeling complete transport aircraft crashes. Single aircraft frames and fuselage section vertical drop tests were modeled and analyzed to obtain comparisons with experimental data and to develop hybrid element crush springs for use in the large CID model. Modifications to DYCAST were made during the study. Predictions of crush and acceleration levels from a symmetric CID model agreed well with data from the CID experiment. The good comparisons achieved with the DYCAST model of the CID indicate the validity of the building-block analysis approach of using results from detailed models of substructure to form hybrid elements for inputs to more complex structures to limit the size of the model and provide a useful prediction tool for crash assessment.

Acknowledgment

The authors acknowledge the support, enthusiasm, and contributions to this paper by the late Robert G. Thomson, former head of the Impact Dynamics Branch at NASA Langley Research Center. His pioneering efforts in full-scale crash testing and leadership in crashworthiness research have provided a solid foundation for researchers in crash dynamics to build upon.

References

[1]Williams, M. S. and Hayduk, R. J., "Vertical Drop Test of a Transport Fuselage Section Located Forward of the Wing," NASA TM-85679, Aug. 1983, pp. 1-55.

[2]Williams, M. S. and Hayduk, R. J., "Vertical Drop Test of a Transport Fuselage Center Section Including the Wheel Wells," NASA TM-85706, Oct. 1983, pp. 1-57.

[3]Fasanella, E. L., Hayduk, R. J., Robinson, M. P., and Widmayer, E., "Analysis of a Transport Fuselage Section Drop Test," NASA CP-2335, 1984, pp. 347-368,.

[4]Hayduk, R. J., Winter, R., Pifko, A. B., and Fasanella, E. L., "Application of the Non-Linear Finite Element Computer Program DYCAST to Aircraft Crash Analysis," *Structural Crashworthiness*, Butterworth & Co., 1983, pp. 282-307.

[5]Hayduk, R. J., compiler, "Full-Scale Transport Controlled Impact Demonstration," NASA CP-2395, 1986, pp. 29-47, 61-123.

[6]Hayduk, R. J., Fasanalla, E. L., and Alfaro-Bou, E., "NASA Experiments Onboard the Controlled Impact Demonstration," SAE Paper 851885, Oct. 1985, pp. 1-11.

[7]Fasanella, E. L., Alfaro-Bou, E., and Hayduk, R. J., "Impact Data from the Controlled Impact Demonstration of a Transport Aircraft," NASA TP-2589, 1986, pp. 1-84.

[8]Soltis, S., Caiafa, C., and Witlin, G., "FAA Structural Crash Dynamics Program Update—Transport Category Aircraft," SAE Paper 851887, Oct. 1985.

[9]*Boeing 707-720 Reference Guide D6-40942*, Boeing Commercial Airplane Co., March 1980.

[10]Fasanella, E. L. and Alfaro-Bou, E., "Vertical Drop Test of a Transport Fuselage Section Located Aft of the Wing," NASA TM-89025, Sept. 1986, pp. 1-24.

[11]Thomson, R. G. and Caiafa, C., "Structural Response of Transport Airplanes in Crash Situations," NASA TM-85654, June 1983, pp.1-97.